ELECTRONIC SUPPORTING INFORMATION

Selective capture of hexavalent chromium from an anion-exchange column of metal organic resin-alginic acid composite

Sofia Rapti,[a] Anastasia Pournara,[a] Debajit Sarma,[b] Ioannis Papadas,[c] Gerasimos S. Armatas,[c] Athanassios C. Tsipis,[a] Theodore Lazarides,[d] Mercouri G. Kanatzidis [e] and Manolis J. Manos*[a]

[a] Department of Chemistry, University of Ioannina, 45110 Ioannina, Greece.

[b]Department of Chemistry, Northwestern University, Evanston, IL 60208.

[c]Department of Materials Science and Technology, University of Crete

71003 Heraklion, Greece.

[d]Department of Chemistry, Aristotle University of Thessaloniki, 54124 Thessaloniki, Greece.

Contents

EXPERIMENTAL SECTION

Materials. All reagents and solvents were commercially available and used as received.

Synthesis of UiO-66-NH_2BDC (as prepared MOR-1). The synthesis was performed as in ref. 11b (main text) but in a larger scale. Specifically, $ZrCl_4$ (0.625gr, 2.7mmol) and NH_2-H_2BDC (0.679gr, 3.75mmol) were dissolved in 75mL DMF and 5mL HCl in a jar. The jar was sealed and placed in an oven operated at 120 ˚C, remained undisturbed at this temperature for 20 h and then was allowed to cool at room temperature. White powder of **UiO-66-NH_2BDC** was isolated by filtration and dried in the air. Yield: 1 g. Note that for the comparative batch sorption **non-protonated MOR-1** was prepared with no addition of acid in the reaction mixture (otherwise the synthesis is as described above) and protonated **MOR-1** was isolated by stirring as-prepared **MOR-1** with 4M HCl solution.

Synthesis of MOR-1-HA composite.

Method A. 0.1 g of sodium alginate (SA) was dissolved in 200 mL of warm water, and then the solution was allowed to cool. A fine suspension of **MOR-1**- SA was formed by adding 1 g of as prepared **MOR-1** to ~ 80 ml of the SA solution. To this suspension, 1 g of $CaCl_2$ was then added with continuous stirring. The composite **MOR-1-CA** immediately precipitated and was isolated by filtration, washed with water and acetone and vacuum dried. Yield: 0.85 g. To prepare the **MOR-1-HA** material, **MOR-1-CA** (0.2 g) is treated with 4 M HCl (50 mL) for ~ 1 h.

Method B. This method is similar with the *A* one, with the difference that HCl solution (final concentration ~ 4 M) is added to the **MOR-1**- SA suspension instead of $CaCl_2$.

Synthesis of UiO-66-HA composite. The preparation of this material was similar with that of **MOR-1-HA** *(method A*), with the exception that UiO-66 MOF was used instead of as-prepared **MOR-1**.

Physical measurements. PXRD diffraction patterns were recorded on a Bruker D8 Advance X-ray diffractometer (CuKa radiation, λ = 1.5418 Å). IR spectra were recorded on KBr pellets in the 4000-400 cm^{-1} range using a Perkin-Elmer Spectrum GX spectrometer. Thermogravimetric analyses (TGA) were performed on a Perkin-Elmer Diamond system. Thermal analysis was conducted from 30 to 780 ^oC in air atmosphere (100 mL min^{-1} flow rate) with a heating rate of 10 ^oC min^{-1}. Energy dispersive spectroscopy (EDS) analyses were performed on a JEOL JSM-6390LV scanning electron microscope (SEM) equipped with an Oxford INCA PentaFET-x3 energy dispersive X-ray spectroscopy (EDS) detector. Data acquisition was performed with an accelerating voltage of 20 kV and 120 s accumulation time. X-ray photoelectron spectroscopy (XPS) was performed on a Perkin Elmer Phi 5400 ESCA system equipped with a Mg Kα x-ray source. Samples were analyzed at pressures between 10^{-9} and 10^{-8} Torr with a pass energy of 29.35 eV and a take-off angle of 45°. All peaks were referred to the signature C_{1s} peak for adventitious carbon at 284.6 eV. Fitting of the peaks has been made by using the software XPSPEAK41. UV/vis Cr(VI) solution spectra and solid state spectra of the materials were obtained on a Shimadzu 1200 PC in the wavelength range of 200-800 nm. N_2 adsorption-desorption isotherms were measured at 77 K on a Quantachrome Nova 3200*e* sorption analyzer. Before analysis, all samples were EtOH-exchanged, activated via supercritical CO_2 drying and then, degassed at 120 ^oC under vacuum (<10^{-5} Torr) for 12 h. The specific surface areas were calculated by applying the Brumauer-Emmett-Teller (BET) method to the branch of isotherms in the 0.05–0.25 relative pressure (P/P_o) range. CO_2 adsorption isotherms were measured at 273 K

using an IGA-003 gravimetric sorption analyzer (Hiden Isochema, UK). The activation of the materials was done as with the N_2 sorption measurements. The pore size distribution plot was obtained from the CO_2 adsorption data using the density functional theory (DFT) method. Inductively Coupled Plasma-Mass Spectroscopy (ICP-MS) analyses were performed using a computer-controlled Thermo Scientific iCAP Q ICP-MS with a quadruple setup equipped with Collision Cell Technology.

Preparation of the column. 50 mg of **MOR-1-CA** composite and 5 g of sand (50-70 mesh SiO_2) was mixed in a mortar and pestle and filled in a glass column (0.7 cm ID column). Prior the ion exchange studies, the column was washed with ~ 50 mL HCl (4 M) solution to convert **MOR-CA** to **MOR-HA** composite which contains protonated amine-functional groups and easily exchangeable Cl^- anions.

Batch ion-exchange studies. A typical ion-exchange experiment of **MOR-1-HA** with $Cr_2O_7^{2-}$ is the following: In a solution of $K_2Cr_2O_7$ (0.4 mmol) in water (10 mL, pH ~ 3), compound **MOR-1-HA** (100 mg, ~ 0.04 mmol of **MOR-1**) was added as a solid. The mixture was kept under magnetic stirring for ≈ 1 h. Then, the polycrystalline material, which had orange(red)-brown color, was isolated by filtration, washed several times with water and acetone and dried in the air.

The Cr(VI) uptake from solutions of various concentrations was studied by the batch method at V:m ~ 1000 mL/g, room temperature and 1 h contact. These data were used for the determination of Cr(VI) sorption isotherms. UV-Vis was used for analysis of dichromate solutions with concentration ≥1 ppm. The solutions with Cr(VI) content less than 1 ppm were analyzed with ICP-MS.

The competitive and variable pH ion exchange experiments were also carried out with the batch method at *V*: *m* ratio (1000) mL/g, room temperature and 1 h contact.

For the determination of the sorption kinetics, Cr(VI) ion-exchange experiments of various reaction times (1-60 min) have been performed. For each experiment, a 10 mL sample of $Cr_2O_7^{2-}$ solution (initial dichromate concentration = 21.6 ppm, pH~3) was added to each vial and the mixtures were kept under magnetic stirring for the designated reaction times. The suspensions from the various reactions were filtrated and the resulting solutions were analyzed for their chromium content with ICP-MS.

Alginic acid was tested for Cr(VI) sorption, showing no Cr(VI) sorption capacity.

Column Ion-Exchange studies

Several bed volumes of the solution are passed through the column and collected at the bottom in glass vials. The solutions with $Cr_2O_7^{2-}$ concentration ≥ 1 ppm were analyzed with UV-Vis, whereas the Cr content of those with smaller concentration was determined with ICP-MS. The regeneration of the column is performed by its treatment with ~ 50 mL of HCl acid (4 M) solution. Then, the column is washed with enough water to remove excess acid. Column containing only sand as stationary phase showed no Cr(VI) sorption capacity.

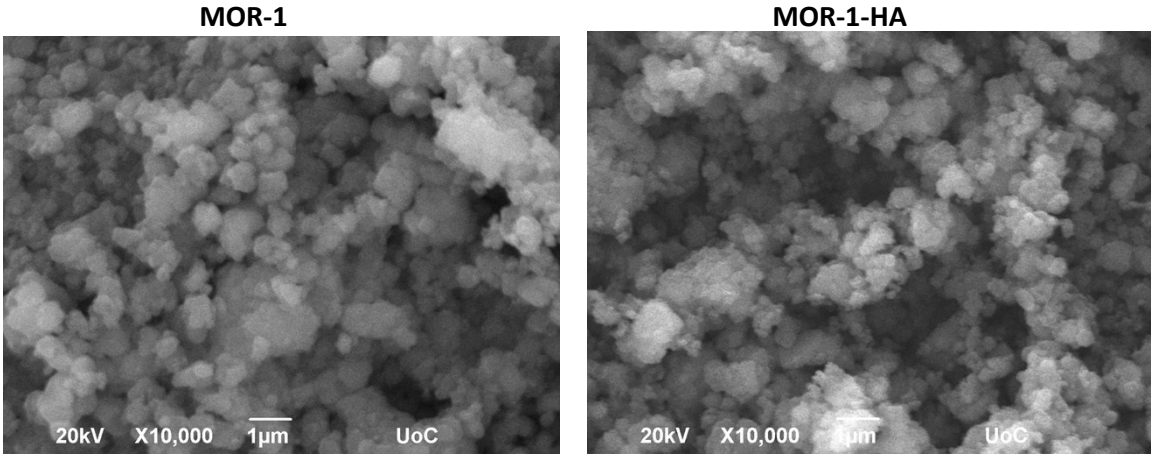

Fig. S1. SEM images of **MOR-1** and **MOR-1-HA**.

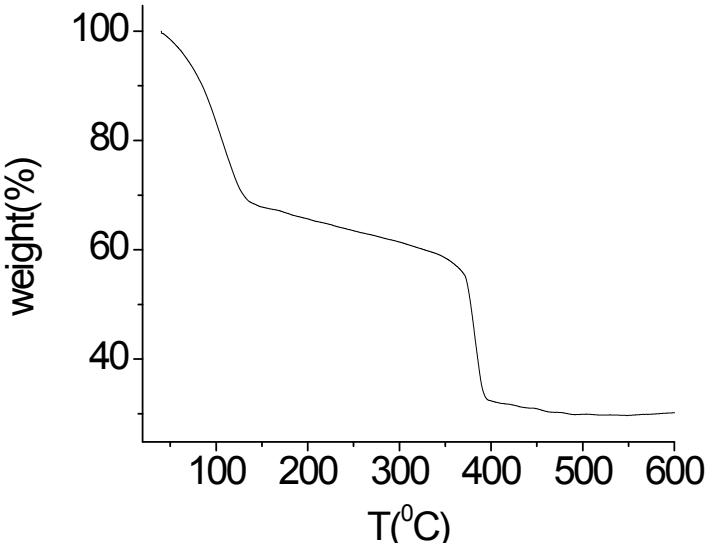

Fig. S2. The TGA data for **MOR-1-HA** measured in air. There is a continuous weight loss starting at 30 ^{0}C and ending at ~ 500 ^{0}C. Considering that a) the final residue (~ 30.2 % of the initial mass) is ZrO_2 (organic molecules including HA are decomposed to CO_2, NO_x, H_2O and Cl^- are released as HCl) and b) the **MOR** initial weight is the 96% of the initial **MOR-1-HA** weight, then the calculated number of water molecules will be ~ 21 (no other type of solvent is present, taking into account the absence of DMF based on the IR data, see Fig. S5).

In more detail: The **MOR-1** is transformed to ZrO_2 according to the equation

$[Zr_6O_4(OH)_4(NH_3^+\text{-}C_8O_4H_3)_6]Cl_6{\cdot}xH_2O \xrightarrow{\text{(air, 600 }^0\text{C)}} 6ZrO_2$ + volatile products (CO_2, H_2O, HCl, NO_x etc).

Thus, one mole of $[Zr_6O_4(OH)_4(NH_3^+\text{-}C_8O_4H_3)_6]Cl_6{\cdot}xH_2O$ yields 6 moles of ZrO_2 or molecular weight (g) of $[Zr_6O_4(OH)_4(NH_3^+\text{-}C_8O_4H_3)_6]Cl_6{\cdot}xH_2O$ (= 1972.9+18x) yields 6 × molecular weight (g) of ZrO_2 (6 × 123.2 = 739.2) .

From the TGA data, we know that 100 g of **MOR-1-HA** composite or 96 g of **MOR-1** (the **MOR** initial weight is the 96% of the initial **MOR-1-HA** weight) are converted to 30.2 g of ZrO_2. Thus, **MOR-1**/ZrO_2 mass ratio = 96/30.2= 3.18 or 1972.9+18x/739.2 = 3.18 and x ~ 21.

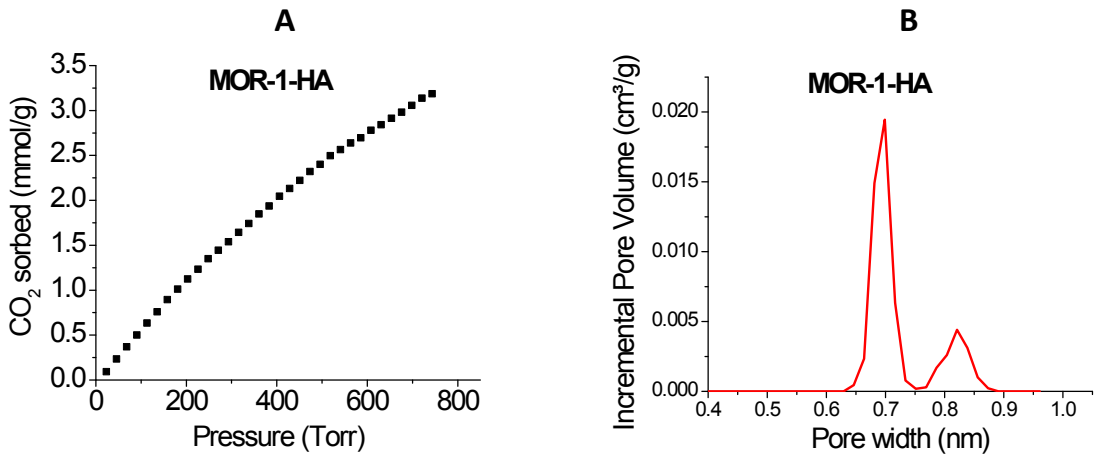

Fig. S3. A) CO_2 adsorption isotherm at 273 K and B) the resultant DFT micropore size distribution (assuming slit-type pores) for **MOR-1-HA**. The DFT analysis of the adsorption data indicates a pore size of ~ 0.7 nm.

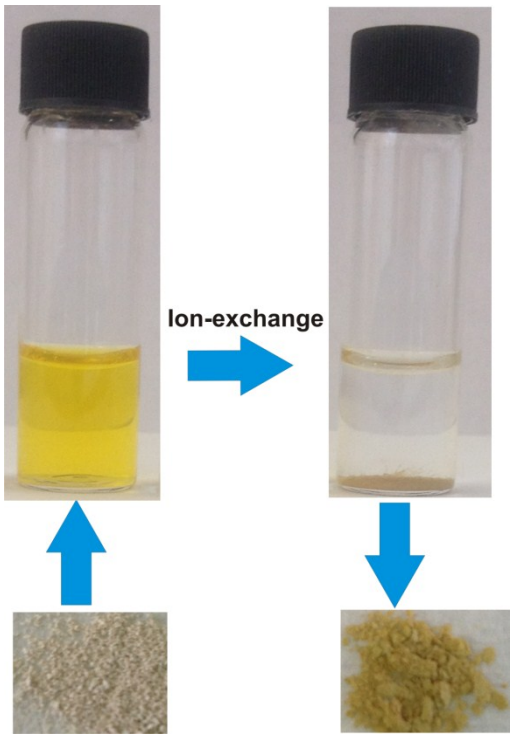

Fig. S4. Decolouration of the dichromate solution (pH~ 3, initial $Cr_2O_7^{2-}$ concentration = 1080 ppm) after its treatment with the **MOR-1-HA** sorbent which also changed color (from cream white to orange(red)-brown).

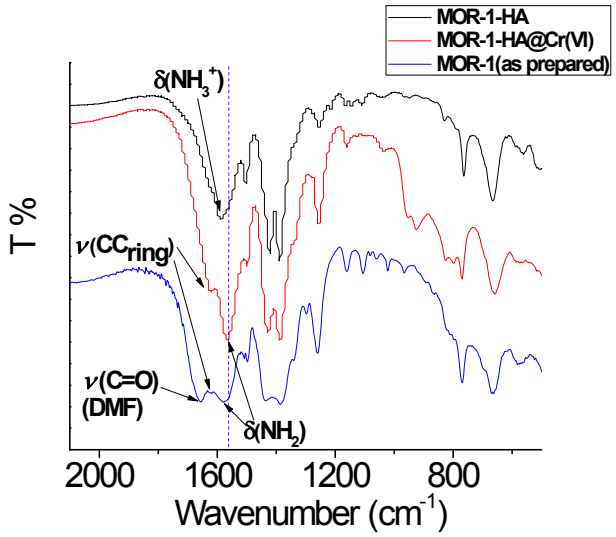

Fig. S5. IR spectra of **MOR-1-HA**, **MOR-1-HA@Cr(VI)** and as prepared **MOR-1**. The assignment of the IR peaks has been made based on the references 17(a), (b) and (c) (main text). Note that no DMF exists in the **MOR-1-HA** composite (absence of the characteristic DMF peak at ~ 1660 cm^{-1}).

Fitting of isotherm data

The fitting of the data with three different isotherm models is given in Table S1 and the graphs are shown in Fig. S6. The models used were the

a) Langmuir $$q = q_m \frac{bC_e}{1 + bC_e} \quad (1)$$

b) Freundlich $$q = K_F C_e^{\frac{1}{n}} \quad (2)$$

c) Langmuir-Freundlich $$q = q_m \frac{(bC_e)^{\frac{1}{n}}}{1 + (bC_e)^{\frac{1}{n}}} \quad (3)$$

where q (mg/g) is the amount of the cation sorbed at the equilibrium concentration C_e (ppm), q_m is the maximum sorption capacity of the sorbent, b (L/mg) is the Langmuir constant related to

the free energy of the sorption, K_F and $1/n$ are the Freundlich constants (see references a) Do, D. D. in *Adsorption Analysis:Equilibria and Kinetics.* pp. 13-17,49-57 (Imperial College Press, 1998); b) Calvet, R. *Environ. Health Persp.* **1989**, *83*, 145-77; c) Arias, M.; Perez-Novo, C.; Lopez, E.; Soto, B. *Geoderma* **2006**, *133*, 151-159; d) Han, R.; Zou, W.; Wang, Y.; Zhu, L. *J. Environ. Radioact.* **2007**, *93*, 127-143).

Table S1. Fitting of the isotherm data for **MOR-1-HA**, **MOR-1**(protonated), **MOR-1**(non-protonated) and **UiO-66-HA** (in the cases that the fitting was not satisfactory no fitting data are provided)

	Langmuir			Freundlich			Langmuir-Freundlich			
Compound	q_e (mg/g)	b (L/mg)	R^2	K_F (L/g)	n	R^2	q_e (mg/g)	b (L/mg)	n	R^2
MOR-1-HA	242±17	0.009±0.003	0.93	30±4	3.3±0.2	0.98	-	-	-	-
MOR-1 (protonated)	247±10	0.025±0.006	0.97	50±10	4.1±0.6	0.96				
MOR-1(non-protonated)	267±23	0.006±0.002	0.95	18±4	2.6±0.3	0.96	-	-	-	-
UiO-66-HA	-	-	-	14±6	2.9±0.6	0.85	129±18	0.017± 0.007	1.0± 0.3	0.93

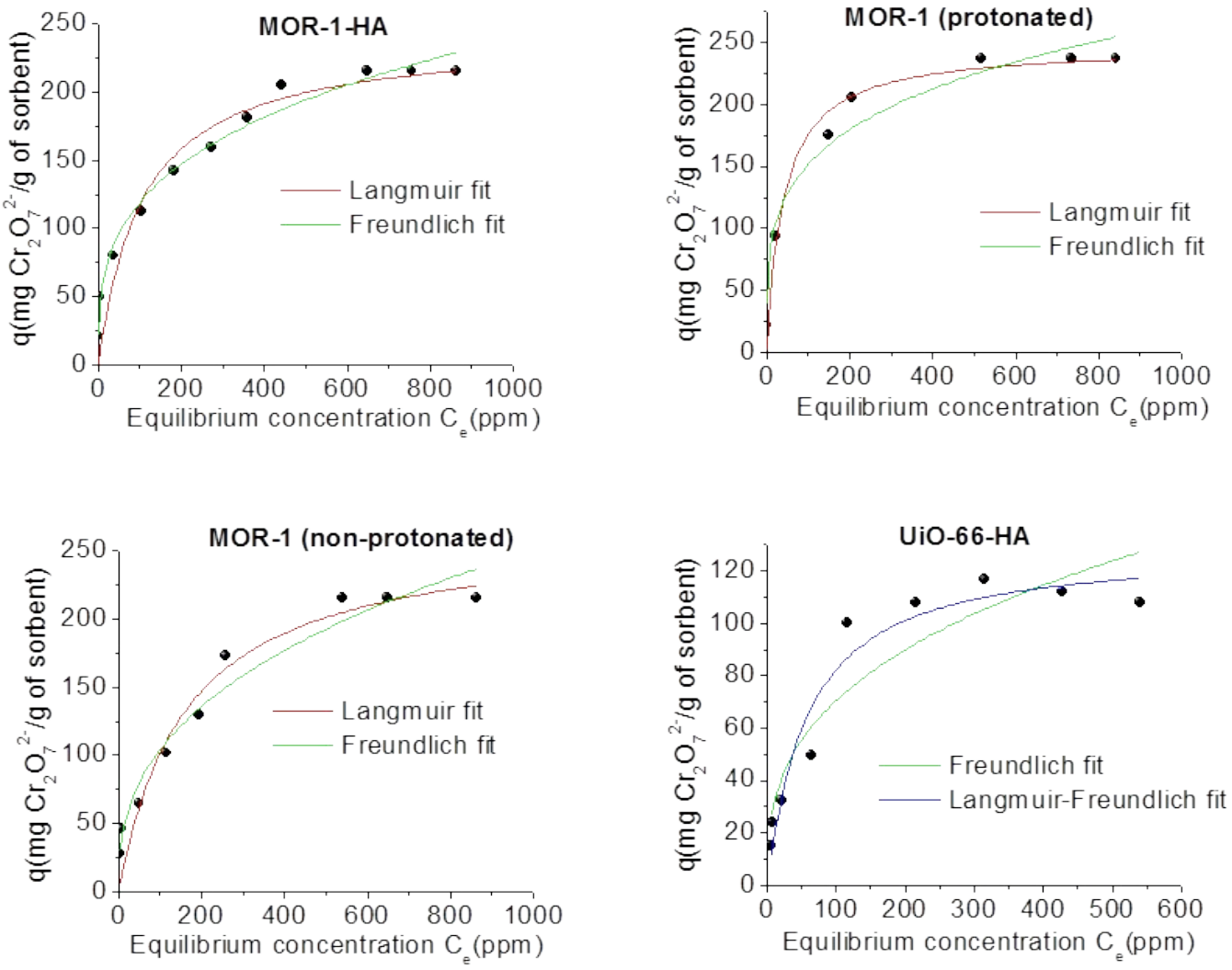

Fig. S6. Cr(VI) isotherm sorption data for **MOR-1-HA**, **MOR-1**(protonated), **MOR-1**(non-protonated) and **UiO-66-HA** with their fitting with the various models.

Estimation of the selectivity of MOR-1-HA for $Cr_2O_7^{2-}$

To estimate the selectivity of **MOR-1-HA** for $Cr_2O_7^{2-}$ versus Cl^-,Br^-, NO_3^- and SO_4^{2-} we plotted the $\log K_d^{Cr_2O_7}$ values versus the logarithmic values of the Cl^-,Br^-, NO_3^- or SO_4^{2-} concentrations (mol/L), Fig. 10b. A linear fitting of the data was attempted using the equation

$$\log K_d^A = \frac{1}{Z_B}\log(K_{A/B}Q^{Z_A}) - \frac{Z_A}{Z_B}\log C_B$$

where A is the ion in trace concentration (i.e. $Cr_2O_7^{2-}$), B is the macro-ion (ion in large concentration, i.e. Cl^-,Br^-, NO_3^- or SO_4^{2-}), Z is the charge of the ion, Q is the absorption capacity of the sorbent (for **MOR-1-HA** = 2.2 meq.Cl^-/g or 1.1 mmol $Cr_2O_7^{2-}$/g) and $K_{A/B}$ is the selectivity coefficient (see reference 15d main text and A. Dyer et. al.. Chem. Mater. 2000, **12**, 3798). The graphs are shown in Fig. S7 and the results of the linear fitting are provided in Table S2.

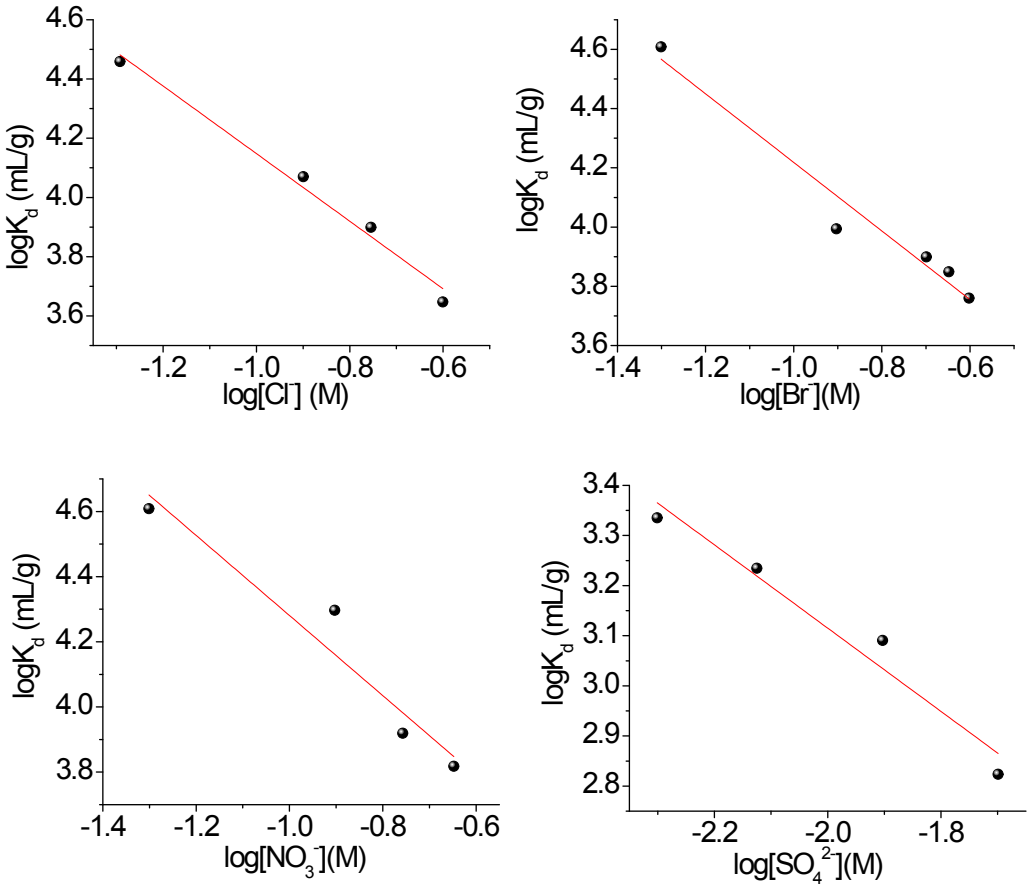

Fig. S7. Plot of the log$K_d{}^{Cr}{}_2{}^{O}{}_7$ values versus the logarithmic values of the Cl^-,Br^-, NO_3^- or SO_4^{2-} concentrations (mol/L) with the linear fitting of the data.

Table S2. The linear fitting data and the $K_{A/B}$ values calculated from these data.

Competitive ion	slope	intercept	$K_{A/B}$	R^2
Cl^-	-1.1	3.00	200	0.98
Br^-	-1.2	3.05	229	0.95
NO_3^-	-1.2	3.06	224	0.90
SO_4^{2-}	-0.8	1.45	159	0.94

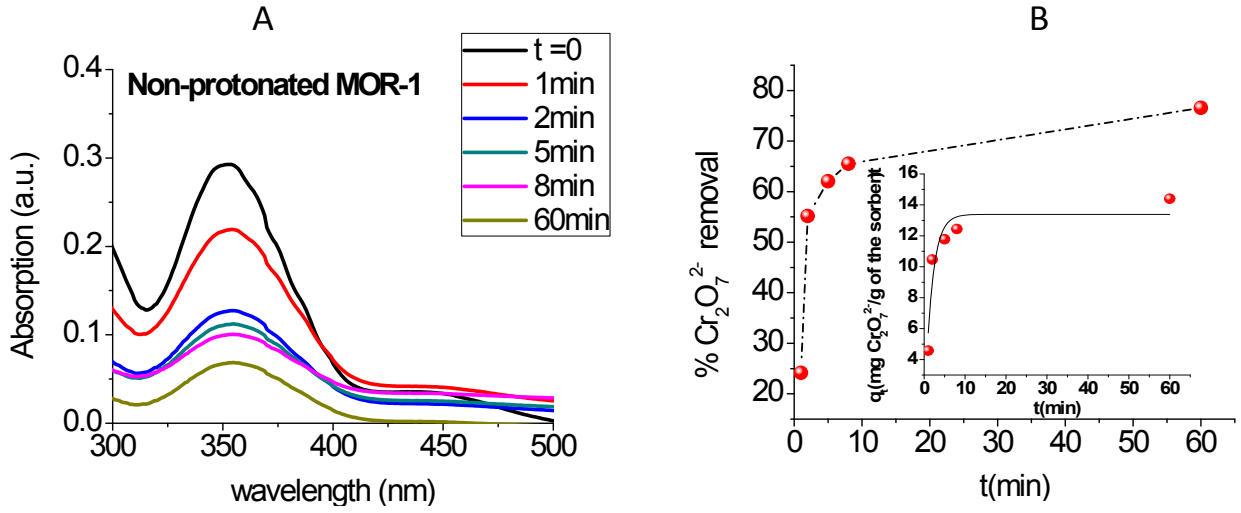

Fig. S8 A) UV-Vis data from the kinetic experiments (initial dichromate concentration = 21.6 ppm, pH~3) for non-protonated **MOR-1** and B) % $Cr_2O_7^{2-}$ removal by non-protonated **MOR-1** vs. time(min). Inset graph: Fitting of the kinetics data with the Lagergren's first order equation (Fitting parameters: q_e= 13.4±0.9 mg/g, K_L = 0.55±0.14 min^{-1}, R^2=0.86)

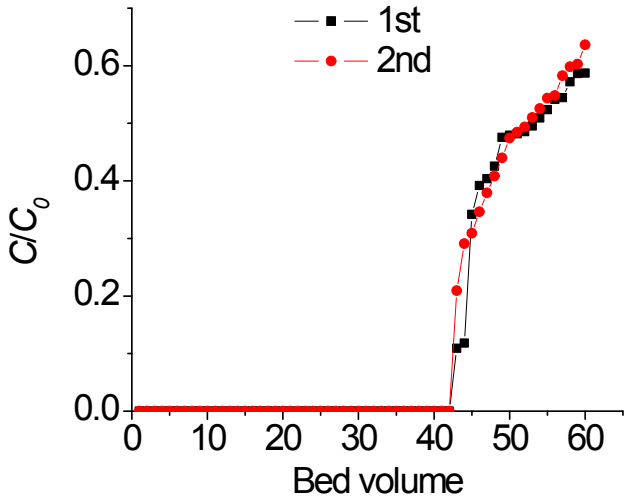

Fig. S9. Breakthrough curves for two column $Cr_2O_7^{2-}$ exchange runs (C= concentration of the effluent, C_0 = initial $Cr_2O_7^{2-}$ concentration ~ 7 ppm (0.03 mM), pH~ 3, flow rate 1 mL/min, one bed volume =3.5 mL, stationary phase **MOR-1-HA**/sand =0.05:5 g) in the presence of large excess of Cl^-, Br^-, NO_3^- (the concentration of each of them ~ 0.3 mM). The lines are only a guide for the eye.

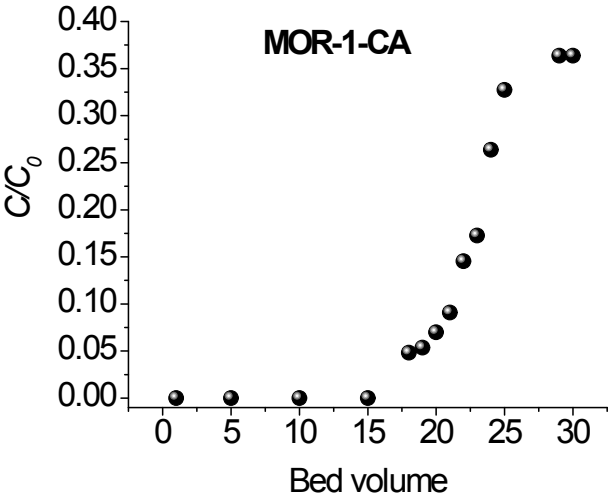

Fig. S10. Breakthrough curve for $Cr_2O_7^{2-}$ sorption by a **MOR-1-CA**/sand column (C= concentration of the effluent, C_0 = initial $Cr_2O_7^{2-}$ concentration ~ 6 ppm, pH~ 3, flow rate 1 mL/min, one bed volume =3.5 mL, stationary phase **MOR-1-CA**/sand =0.05:5 g).

Computational Details

Geometry optimizations, without symmetry constrains, were performed using the dispersion–corrected wB97XD density functional[1] in combination with the Def2-TZVPPD basis set for all elements.[2] All calculations were performed for aqueous solutions of the interacting species using the Polarizable Continuum Model (PCM) for solvation as implemented in the Gaussian 09 program suite.[3] The computational protocol used is denoted as wB97XD/Def2-TZVPPD/PCM. All stationary points were verified as minima (number of imaginary frequencies NImag=0).

(1) Chai, J.-D.; Martin Head-Gordon, M. *Phys. Chem. Chem. Phys.* **2008**, *10*, 6615–6620.

(2) (a) Rappoport, D.; Furche, F. *J. Chem. Phys.* **2010**, *133*, 134105. (b) EMSL basis set exchange, https://bse.pnl.gov/bse/portal, accessed 26-06-2015.

(3) Frisch, M. J.; Trucks, G. W.; Schlegel, H. B.; Scuseria, G. E.; Robb, M. A.; Cheeseman, J. R.; Scalmani, G.; Barone, V.; Mennucci, B.; Petersson, G. A.; Nakatsuji, H.; Caricato, M.; Li, X.; Hratchian, H. P.; Izmaylov, A. F.; Bloino, J.; Zheng, G.; Sonnenberg, J. L.; Hada, M.; Ehara, M.; Toyota, K.; Fukuda, R.; Hasegawa, J.; Ishida, M.; Nakajima, T.; Honda, Y.; Kitao, O.; Nakai, H.; Vreven, T.; Montgomery, J. A., Jr.; Peralta, J. E.; Ogliaro, F.; Bearpark, M.; Heyd, J. J.; Brothers, E.; Kudin, K. N.; Staroverov, V. N.; Kobayashi, R.; Normand, J.; Raghavachari, K.; Rendell, A.; Burant, J. C.; Iyengar, S. S.; Tomasi, J.; Cossi, M.; Rega, N.; Millam, M. J.; Klene, M.; Knox, J. E.; Cross, J. B.; Bakken, V.; Adamo, C.; Jaramillo, J.; Gomperts, R.; Stratmann, R. E.; Yazyev, O.; Austin, A. J.; Cammi, R.; Pomelli, C.; Ochterski, J. W.; Martin, R. L.; Morokuma, K.; Zakrzewski, V. G.; Voth, G. A.; Salvador, P.; Dannenberg, J. J.; Dapprich, S.; Daniels, A. D.; Farkas, Ö.; Foresman, J. B.; Ortiz, J. V.; Cioslowski, J.; Fox, D. J., Gaussian 09, Revision **D.01**, Gaussian, Inc., Wallingford CT, 2009.

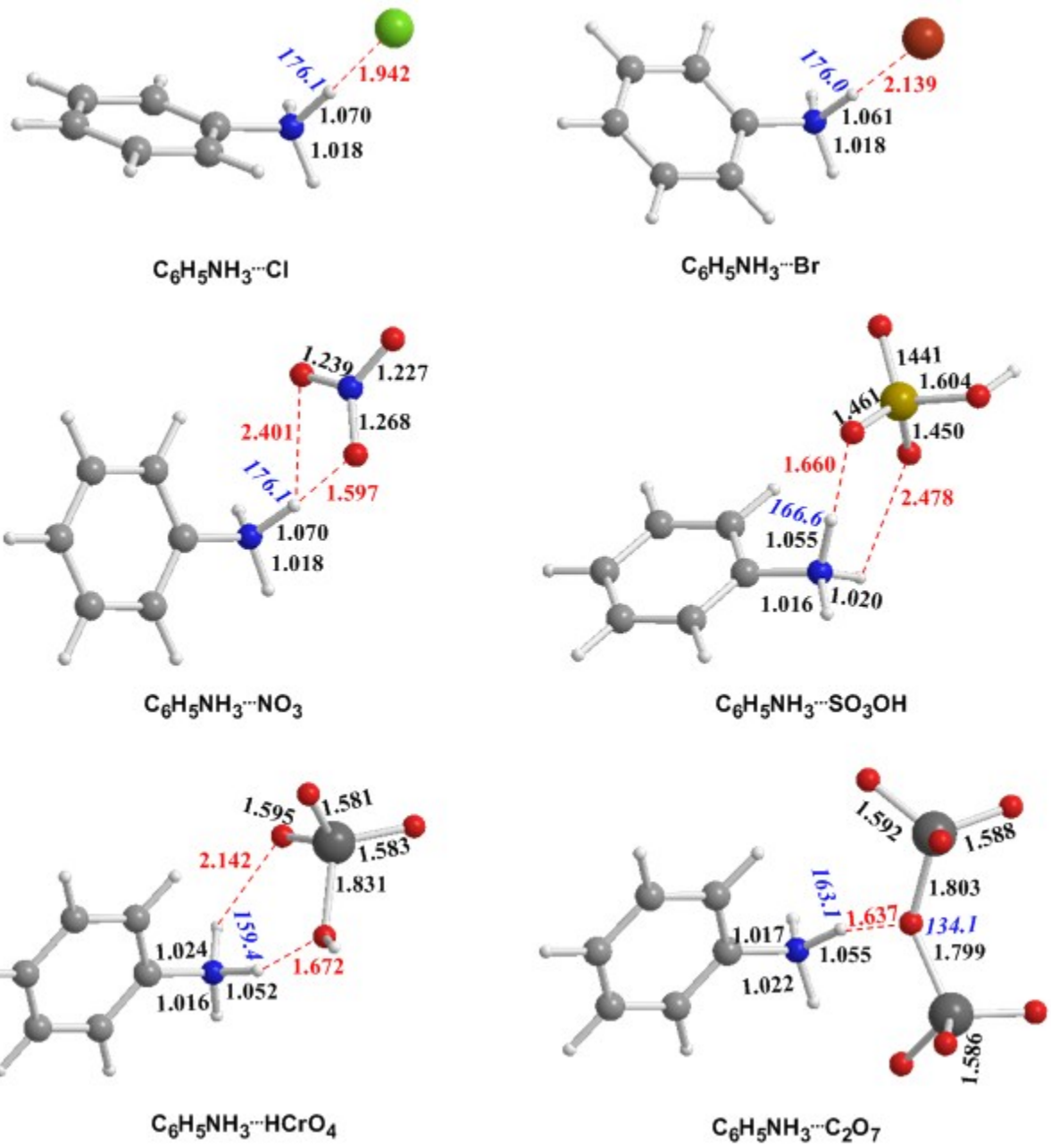

Fig. S11. Optimized geometries of $Cr_2O_7^{2-}$, $HOCrO_3^-$, Cl^-, Br^-, NO_3^-, $HOSO_3^-$ and SO_4^{2-} anions interacting with the $[Zr_6O_4(OH)_4(NH_3^+\text{-BDC})_6]Cl_6$-HA (**MOR-1-HA**), represented by the simple anilinium Ar-NH_3^+ cation calculated at the wB97XD/Def2-TZVPPD level of theory.

The anions A studied are associated with the anilinium Ar-NH_3^+ cation via formation of A···H-N hydrogen bonds. For the $HOCrO_3^-$ and $Cr_2O_7^{2-}$ anions the hydroxyl- and bridging oxygen atoms

participate in the formation of the O···H-N hydrogen bonds. These atoms bear higher negative natural atomic charges amounted to -0.786 and -0.554 |e| respectively as compared to the negative natural atomic charges on the terminal O atoms which are -0.423 and -0.427 |e| respectively. In contrast to $HOCrO_3^-$, the $HOSO_3^-$ anion forms hydrogen bonds between the terminal than the hydroxyl- oxygen atoms, since the terminal O atom bears higher negative natural atomic charge (-1.042 |e|) than the hydroxy- oxygen atom (-0.927 |e|). The estimated interaction energies found in the range of 9.9 – 15.5 kcal/mol are characteristic of weak interactions involving hydrogen bonds and dispersion forces as well.

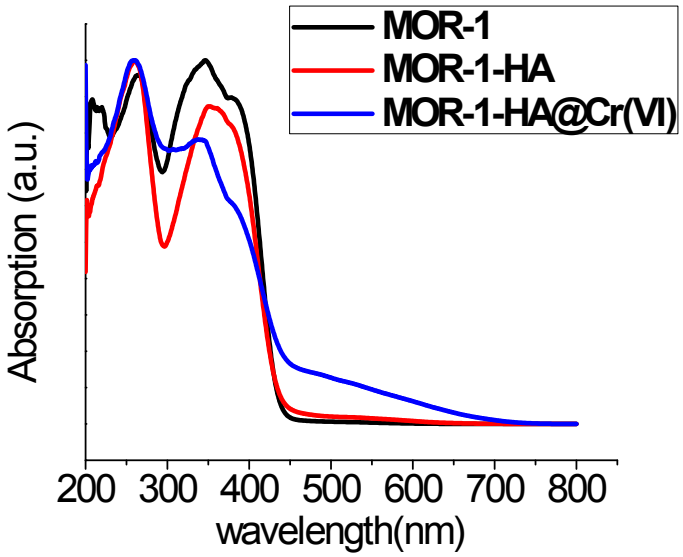

Fig. S12. Solid state UV-Vis spectra for **MOR-1** (as prepared), **MOR-1-HA** and **MOR-1-HA@Cr(VI)**.

Table S3 Cartesian coordinates and energetic data.

$PhNH_3^+$

```
N,0,-4.2085728238,0.0060808627,0.0078282909
C,0,-5.6830199756,0.0018790102,0.0061410027
C,0,-6.3470384482,-1.2140614484,0.0073684878
C,0,-7.7394487733,-1.2071754232,0.0058816693
C,0,-8.4328583021,-0.0008509293,0.0031803151
C,0,-7.7400367416,1.2082490553,0.0019794279
C,0,-6.3495189458,1.2192393807,0.0034947325
H,0,-3.8269613443,0.4773357486,-0.8168528555
H,0,-3.8311115922,-0.9440379419,0.009004074
H,0,-5.7995041129,-2.1506307133,0.0094331316
H,0,-8.2767229775,-2.1485329802,0.0069782444
H,0,-9.5171392876,-0.0013233131,0.0021678866
H,0,-8.2804839029,2.1478390483,-0.0001616383
H,0,-5.8012327511,2.1552602344,0.0027239265
H,0,-3.8287500212,0.4790294093,0.8326333046
Sum of electronic and zero-point Energies=          -287.834547
Sum of electronic and thermal Energies=             -287.828712
Sum of electronic and thermal Enthalpies=           -287.827768
Sum of electronic and thermal Free Energies=        -287.863966
```

$PhNH_3Cl$

```
N,0,0.4725957497,0.2318601357,0.7173282623
C,0,0.2464554993,0.135480027,-0.7218909342
C,0,0.1373141727,1.2877424151,-1.4751563514
C,0,-0.0953638955,1.176058644,-2.8383388744
C,0,-0.2156358258,-0.0746374218,-3.4242527571
C,0,-0.1059656705,-1.2208699379,-2.6487819948
C,0,0.1246297909,-1.1216373736,-1.2862991703
H,0,-0.318625346,-0.2483458353,1.2542888954
H,0,0.5170241161,1.2000730475,1.0241073842
H,0,0.2324568188,2.2606267251,-1.0114131005
H,0,-0.1813702138,2.070634694,-3.4390360441
H,0,-0.3963248706,-0.1576836588,-4.4870516684
H,0,-0.2021641797,-2.1969343281,-3.1033488073
H,0,0.2055048443,-2.00791459,-0.6715861367
H,0,1.3464470904,-0.2126659787,0.9907255996
Cl,0,-1.7994780805,-1.1657865643,2.1122056976
Sum of electronic and zero-point Energies=          -748.339916
Sum of electronic and thermal Energies=             -748.332144
Sum of electronic and thermal Enthalpies=           -748.331200
Sum of electronic and thermal Free Energies=        -748.374334
```

$PhNH_3Br$

N	0.075805351622	-0.610284923338	1.457555277014
C	-1.125254895903	-0.283883351817	0.692066425365
C	-1.715040664351	-1.264990528757	-0.081902685519
C	-2.835993468011	-0.939101861879	-0.830212010769
C	-3.345940477977	0.350406795368	-0.797713494790
C	-2.734738483344	1.321805292613	-0.018168422989
C	-1.612828768246	1.008780243023	0.733452496466
H	0.948213038858	-0.376359847577	0.901450975748
H	0.115353523418	-1.599843919102	1.689144222217
H	-1.312512900357	-2.269012108787	-0.101730240115
H	-3.310070643663	-1.697852121412	-1.436836629813
H	-4.222355462516	0.598872997164	-1.380112613294
H	-3.130345324467	2.327382744542	0.009127083587
H	-1.129610053669	1.761304392895	1.342290590093
H	0.118364794379	-0.091352347469	2.331814585411
Br	2.617567434229	0.127801544531	-0.336908558610

Sum of electronic and zero-point Energies=	-2862.348579
Sum of electronic and thermal Energies=	-2862.340585
Sum of electronic and thermal Enthalpies=	-2862.339641
Sum of electronic and thermal Free Energies=	-2862.384722

$PhNH_3NO_3^-$

N	0	-0.464917206	-1.1177251153	-0.3235330409
C	0	0.890969107	-0.6195347113	-0.1097691352
C	0	1.0681455814	0.4413090115	0.760518301
C	0	2.3483210916	0.9318817365	0.9606400367
C	0	3.4262176165	0.365729363	0.2936198534
C	0	3.2264767486	-0.6947770558	-0.5768813017
C	0	1.9493790334	-1.1961362975	-0.784102851
H	0	-0.4875173815	-1.859171233	-1.0176851476
H	0	-1.1118428979	-0.3242646336	-0.6373770061
H	0	0.2154911138	0.871775727	1.2690265791
H	0	2.5018976807	1.7598973045	1.6385706201
H	0	4.4231848311	0.7529657219	0.4526334637
H	0	4.0635848818	-1.1373019182	-1.0984818958
H	0	1.7871794012	-2.023994849	-1.4617515029
H	0	-0.8644493195	-1.4864477566	0.5370268536
O	0	-2.3331127399	0.7921840373	1.1021283942
N	0	-2.5694460251	1.3632826713	0.027835475
O	0	-2.0176183088	0.9313792344	-1.0284562884
O	0	-3.3200034886	2.3322726228	-0.0381458472

Sum of electronic and zero-point Energies=	-568.429002
Sum of electronic and thermal Energies=	-568.418672
Sum of electronic and thermal Enthalpies=	-568.417728
Sum of electronic and thermal Free Energies=	-568.467809

$PhNH_3HOSO_3^-$

N,0,-2.3198764302,0.3270270186,0.4163902057
C,0,-0.8742268125,0.2175764374,0.2308079397
C,0,-0.1095737379,1.3638320146,0.3515524255
C,0,1.2586624324,1.2735126668,0.1531179729
C,0,1.8402635399,0.053096869,-0.1624705474
C,0,1.0543259259,-1.0830498013,-0.2797569285
C,0,-0.3169040882,-1.0061038521,-0.0826413336
H,0,-2.7713826965,-0.5830777104,0.4301259794
H,0,-2.7503566906,0.9199704523,-0.342207462
H,0,-0.5807687471,2.3065157932,0.5969071627
H,0,1.8701867653,2.1601746524,0.2455324066
H,0,2.908543473,-0.0117426242,-0.3164113875
H,0,1.5045081372,-2.0349185716,-0.5243762074
H,0,-0.935936986,-1.8890222761,-0.1718785429
H,0,-2.5478819179,0.8097450606,1.2851276777
O,0,-3.3012198152,2.1462342557,-1.3162448993
S,0,-3.4701128331,3.3644586986,-0.5274148953
O,0,-2.9945211772,4.5586329197,-1.17769354
O,0,-5.0685078773,3.4808970963,-0.4696540688
O,0,-3.0161808061,3.2019508953,0.8397068465
H,0,-5.3148396577,4.3108900051,-0.0488188041
Sum of electronic and zero-point Energies= -987.848273
Sum of electronic and thermal Energies= -987.836243
Sum of electronic and thermal Enthalpies= -987.835299
Sum of electronic and thermal Free Energies= -987.889368

$PhNH_3SO_4^{2-}$

N	-0.68703600	1.58818300	0.97807200
C	-1.69395400	0.69775900	0.55245300
C	-1.67753600	-0.63181200	0.96510400
C	-2.61942400	-1.52333900	0.47520100
C	-3.59156100	-1.10277000	-0.42333200
C	-3.60837900	0.22436200	-0.83208900
C	-2.66719000	1.12149300	-0.35186700
H	-1.00158000	2.54270900	1.06817400
H	0.68409300	1.38407300	-0.20079400
H	-0.91360900	-0.96558900	1.65922900
H	-2.59259800	-2.55476400	0.80469100
H	-4.32437600	-1.80104100	-0.80234900
H	-4.35955200	0.56794000	-1.53048400
H	-2.67723400	2.15218300	-0.68395800
H	-0.22540400	1.29259600	1.82638400
O	1.39608800	1.17838400	-0.85951100
S	2.13537300	-0.17883300	-0.43661600
O	1.46060600	-1.24788600	-1.15448300
O	3.50196100	0.02638600	-0.88116300
O	1.98251100	-0.27113400	1.00694000

$PhNH_3HOCrO_3^-$

N,0,-2.3927558953,0.6384339786,0.2412723516
C,0,-0.9792693667,0.3226755547,0.0510594286
C,0,-0.0182065058,1.257953438,0.3793497118
C,0,1.3187240975,0.9294749036,0.2062998164
C,0,1.6721521226,-0.3169628996,-0.2871507051
C,0,0.6895678148,-1.2424825391,-0.6115772373
C,0,-0.6487950604,-0.9268089461,-0.4425432925
H,0,-2.9136728625,0.5762621528,-0.6375617664
H,0,-2.5290388856,1.5659718581,0.6319253859
H,0,-0.2999745636,2.2294236526,0.7635122983
H,0,2.0813833123,1.6525061803,0.4594241863
H,0,2.7152961315,-0.5688129909,-0.4194440323
H,0,0.9631446794,-2.2150225982,-0.9961042003
H,0,-1.4235252913,-1.640365137,-0.6907339373
H,0,-2.8497040596,-0.077126671,0.8620023834
O,0,-4.2402061987,-0.9803625782,-1.2737880002
Cr,0,-4.5026993298,-2.1228041933,-0.1918614711
O,0,-3.7807337378,-3.4737600365,-0.584227163
O,0,-3.712963745,-1.4367039465,1.3108510889
O,0,-6.047167776,-2.3527901422,0.0661530014
H,0,-3.4185548802,-2.0800990401,1.9569421529
Sum of electronic and zero-point Energies= -1634.161428
Sum of electronic and thermal Energies= -1634.148501
Sum of electronic and thermal Enthalpies= -1634.147557
Sum of electronic and thermal Free Energies= -1634.203263

$PhNH_3Cr_2O_7^{2-}$

N,0,-0.943124566,-0.5740602451,-0.8004086236
C,0,-0.0580532295,-1.0619100457,0.255092906
C,0,-0.6245493772,-1.5040207617,1.4359734064
C,0,0.2106061328,-1.9728417455,2.4387676125
C,0,1.5853246792,-1.9900356888,2.2519721104
C,0,2.1328517654,-1.5370596531,1.0603172865
C,0,1.3084590144,-1.0679397458,0.0490364488
H,0,-0.4973195087,0.156164764,-1.3588716254
H,0,-1.7884699892,-0.0985668357,-0.3855008342
H,0,-1.6993422206,-1.4773909897,1.5704788934
H,0,-0.2167708853,-2.3208456099,3.3688528443
H,0,2.2324496808,-2.3537800311,3.0382684019
H,0,3.2039570727,-1.5454389405,0.9143644892
H,0,1.7270157698,-0.710943591,-0.882566201
H,0,-1.247025483,-1.319210395,-1.4225031886
O,0,-0.8979793627,2.2846366857,-1.1619429809
O,0,-1.8046220074,3.486284379,0.9934562268
O,0,-3.2934755364,3.3689171939,-1.1452541575

```
Cr,0,-2.1888565508,2.6268457388,-0.2825625772
O,0,-2.8080426134,1.0204242618,0.2378000782
O,0,-4.051780474,-1.0900181107,1.3861215106
O,0,-5.5604832448,0.7812498067,0.3402430698
O,0,-4.2793271983,1.2397837064,2.5694340785
Cr,0,-4.2469052077,0.475799443,1.1783807651
Sum of electronic and zero-point Energies=          -2903.958857
Sum of electronic and thermal Energies=             -2903.941715
Sum of electronic and thermal Enthalpies=           -2903.940771
Sum of electronic and thermal Free Energies=        -2904.008246
```

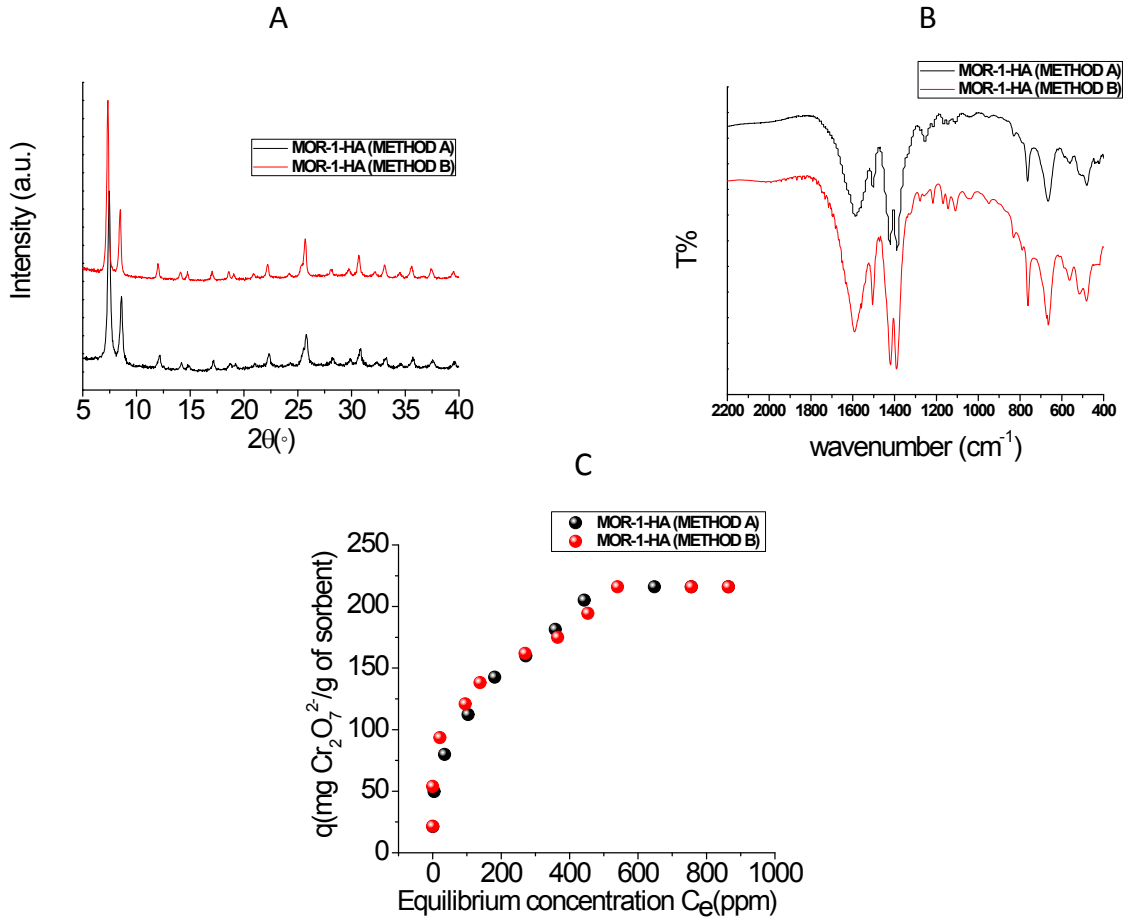

Fig. S13. PXRD (A), IR (B) and (C) Cr(VI) isotherm sorption data for **MOR-1-HA** material prepared with method B vs. the corresponding data for **MOR-1-HA** prepared with method A. These data indicate that the material prepared with method B shows quite similar structural characteristics and almost identical ion-exchange properties with those of the composite isolated with method A.